Cooperative effect of multiple hydrogen bonding involving the nitro group: solid state dimeric self-assembly of *o*-, *m*- and *p*-hydroxyphenyl-2,4-dinitrophenylhydrazones

Beata Szczęsna and Zofia Urbańczyk-Lipkowska

Institute of Organic Chemistry, Polish Academy of Sciences, 01-224 Warsaw, Poland. E-mail: ocryst@icho.edu.pl; Fax: +22 632 6681

Received (in Strasbourg, France) 21st June 2001, Accepted 8th October 2001
First published as an Advance Article on the web 24th January 2002

Solid state studies of *o*-, *m*-, and *p*-hydroxyphenyl-2,4-dinitrophenylhydrazones: **1**, **2**, **3** and **4** (**3**·0.5 MeCN) revealed dimeric self-assembly of molecules. A pattern of two NH···O_2N and up to six CH···O_2N intermolecular hydrogen bonds creates cohesive forces between two molecules of the dimer. Push–pull effects of numerous weak interactions generate non-bonding contacts between negatively charged O atoms of the *o*-NO_2 groups in the range 2.683(2)–2.894(3) Å, far below the sum of van der Waals radii. Both the presence of OH groups and MeCN molecules in the crystals does not interfere much with dimer formation. Low temperature X-ray data collected for compound **1** provided evidence that due to the involvement of the *o*-NO_2 group oxygen in a new type of intramolecular, resonance-assisted hydrogen-bonded system (RAHB), the phenyl ring has a 2,5-diene geometry. The packing patterns observed in crystals of compounds **1**–**4** are explained as a result of competition between in-plane hydrogen bonding and inter-planar interactions dominated by π–π stacking and dipole–dipole overlap. FT-IR data confirm aggregation in solution. Another examples of short contacts between nitro group oxygens found in the Cambridge Crystallographic Database are discussed.

Rational design of organic materials *via* application of non-covalent interactions has been a long time interest for solid state chemists. The selectivity of intermolecular interactions observed between complementary chemical entities in crystals has allowed to define the major types such as hydrogen bonds, ionic forces, π–π stacking, *etc*., and to characterise the geometry and topology of the basic recognition patterns. These were then included into the list of so-called "supramolecular synthons".[1–3] Although the list of supramolecular synthons is not completed yet, knowledge of the above motifs has some practical value. It gives the opportunity to design simple building blocks and to control the construction of new solid state organic and organometallic materials with desired properties, employing crystal engineering techniques.[4–8] In real crystals however, single motifs are rare. Usually, competition between various intra- and intermolecular forces influences both molecular geometry and crystal packing. As knowledge of molecular recognition motifs is critical in crystal engineering, *ab initio* crystal modelling[9] and understanding of biological processess, we undertook structural studies on molecular recognition in the case where possible competition between hydrogen bonding and interactions between π-electron systems can occur.[10]

Molecular recognition of a nitro group in the context of crystal engineering has recently attracted much attention. Early work of Etter *et al.* on molecular recognition of nitroanilines revealed that amine protons are recognized by nitro groups preferably *via* **a** and **b** patterns, shown in Scheme 1.[11] Further studies involving recognition of single hydrogen OH and NH donor groups showed that, contrary to crystal structures of nitroanilines, pattern **c** predominates.[12–14]

Rationalisation of this recognition behaviour came both from *ab initio* calculations and analysis of crystal structures stored in the Cambridge Crystallographic Database.[15] It has been emphasized that although the nitro group is a weak

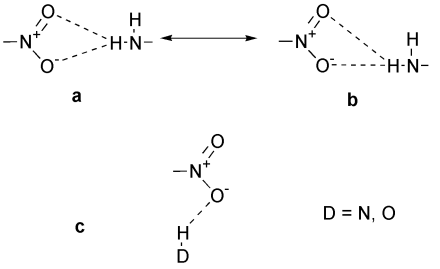

Scheme 1

acceptor, its recognition pattern is a combination of electronic properties and the directionality of the oxygen atom lone pairs and can be modulated by the character of the H-atom donating groups. Indeed, our solid state studies on the conformation of picrate ion showed that the nitro group is very sensitive to the chemical environment and involvement in even weak hydrogen bonds changes both the conformation and resonance structure of the phenyl ring.[10] Recently, charge optimisation methods used for modelling electrostatic interactions during ligand binding to a chorismate mutase has shown that replacement of carboxylate ion with an isosteric nitro group improves binding energy by 2–3 kcal mol^{-1}. Whereas both groups maintain similar hydrogen bonding patterns with neighbouring H-atom donors, the nitro group is less solvated.[16]

Our present subjects, aromatic 2,4-dinitrophenylhydrazones, contain an elongated π-electron system, whose polarity can be easily adjusted by introducing electron-donating and electron-withdrawing groups on the aromatic carbons. This allows preparation of highly polarisable molecules with preferential crystal packing due to overlapping of the π-electron systems. Substitution by proton-donor or proton-acceptor groups

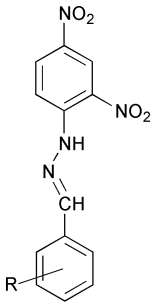

R:	compound
o-OH	**1**
m-OH	**2**
p-OH	**3**
p-OH . 0.5 MeCN	**4**

Scheme 2

allows construction of simple models expressing quite complex recognition patterns in which, due to the planarity of the molecules, possible hydrogen bonds should form planar networks with strong interplanar interactions between dipoles and π-electron systems. The present study concentrates on the preparation and structural investigation of four 2,4-dinitrophenylhydrazones shown in Scheme 2: **1**, **2**, **3** and **4** (**3**·0.5 MeCN) in which a nitro group located in the *ortho* position should be involved in an intramolecular NH···ON hydrogen bond. Competition between various non-bonded interactions found in crystal and in solution will be discussed. Low temperature data of a new type of resonance-assisted hydrogen-bonded system involving NH and *o*-NO_2 groups and its influence on molecular geometry and crystal packing will be discussed. Discussion of crystal packing peculiarities will be enriched by a survey of the Cambridge Crystallographic Database.

Experimental

Compound preparation and characterisation

Title compounds have been prepared by slow addition of 1 mmol of 2,4-dinitrophenylhydrazine dissolved in 100 ml of MeOH and the respective 2-, 3- or 4-hydroxybenzaldehyde dissolved in 50 ml of MeOH. The mixture was stirred for 3–4 h with heating at *ca.* 50 °C and then left for crystallisation. After 5–14 days orange to red crystals of **1**, **2**, and **3** appeared. They were recrystallised from MeOH or MeCN (**4** is **3**·0.5 MeCN) and then characterised by melting point, FT-IR, ^{1}H and ^{13}C NMR and X-ray crystallography. Compounds **1**–**3** have been prepared previously in solution[17–19] and under solventless conditions.[20]

Solution and solid state FT-IR spectra were recorded using a Perkin Elmer 16400 Fourier transform spectrometer in KBr or $CHCl_3$ using compounds dried overnight in vacuum.

Crystal structure determination

X-Ray diffraction experiments were performed on a Nonius BV MACH3 diffractometer (compounds **2**–**4**) or Nonius BV Kappa CCD system (compound **1**). Details of data collection and structure refinement are shown in Table 1. Lattice constants for compounds **2**–**4** were determined by a least-squares fit of the setting angles of 25 reflections and for compound **1** by a fit of all reflections. Intensities of three standard reflections measured every 2 h did not show significant fluctuations for any of the four compounds. The structures were solved by SHELXS97[21] and refined with SHELXL97[22] programs. Hydrogens attached to carbon atoms were included at their geometrical positions and refined in the riding mode. Amine and hydroxyl protons were located from $\Delta\rho$ maps and refined with isotropic temperature factors and no restrictions put on the D–H distance.

CCDC reference numbers 177492–177495. See http://www.rsc.org/suppdata/nj/b1/b105498h/ for crystallographic data in CIF or other electronic format.

Cambridge Crystallographic Database (CCD) searches

All searches reported here were of the CCD release dated May 2000 (224 000 entries). The search criteria were error and disorder-free structures with *R* factors less then 0.1. Only intermolecular $NO_2\cdots NO_2$ interactions were considered.

Results and discussion

Resonance-assisted hydrogen bonding

Fig. 1–4 show ORTEP diagrams of the title compounds with some details of non-bonding distances in the least-squares plane of the molecules and perpendicularly to that plane. Table 2 shows selected bond lengths and bond angles found in compounds **1**–**4**. Significantly different N–O bond lengths in the *ortho* positioned NO_2 group characterise the molecular geometry in this class of compounds. Moreover, C–C bond lengths and valence angles in the 2,4-dinitrobenzene moiety

Table 1 Selected X-ray data collection and refinement parameters for **1**–**4**

	1	**2**	**3**	**4**
Empirical formula	$C_{13}H_{10}N_4O_5$	$C_{13}H_{10}N_4O_5$	$C_{13}H_{10}N_4O_5$	$C_{15}H_{13}N_5O_5$
Formula weight	302.25	302.25	302.25	322.78
T/K	200(2)	293(2)	293(2)	293(2)
Crystal system	Monoclinic	Monoclinic	Monoclinic	Monoclinic
Space group	$P2_1/n$	$P2_1/n$	$P2_1/n$	$C2/c$
a/Å	13.767(4)	9.790(1)	8.430(4)	12.002(2)
b/Å	4.353(1)	14.035(1)	6.186(7)	9.175(2)
c/Å	21.118(7)	9.823(1)	24.715(1)	27.266(5)
β/°	90.407(1)	101.32(3)	91.49(1)	102.15(3)
U/Å^3	1265.52(6)	1323.4(2)	1288.29(17)	2935.2(10)
Z	4	4	4	8
μ/mm^{-1}	0.125	1.024	1.052	0.972
Total reflect.	2973	2913	2665	1434
Unique reflect.	2973	1611	2606	1434
R(int)	0.0	0.041	0.046	0.0
R_1 [$I > 2\sigma(I)$]	0.0478	0.0543	0.0566	0.0467
wR_2 [$I > 2\sigma(I)$]	0.0943	0.1337	0.1324	0.1099
R_1(all data)	0.1049	0.0588	0.0892	0.0473
wR_2(all data)	0.1065	0.1372	0.1563	0.1119

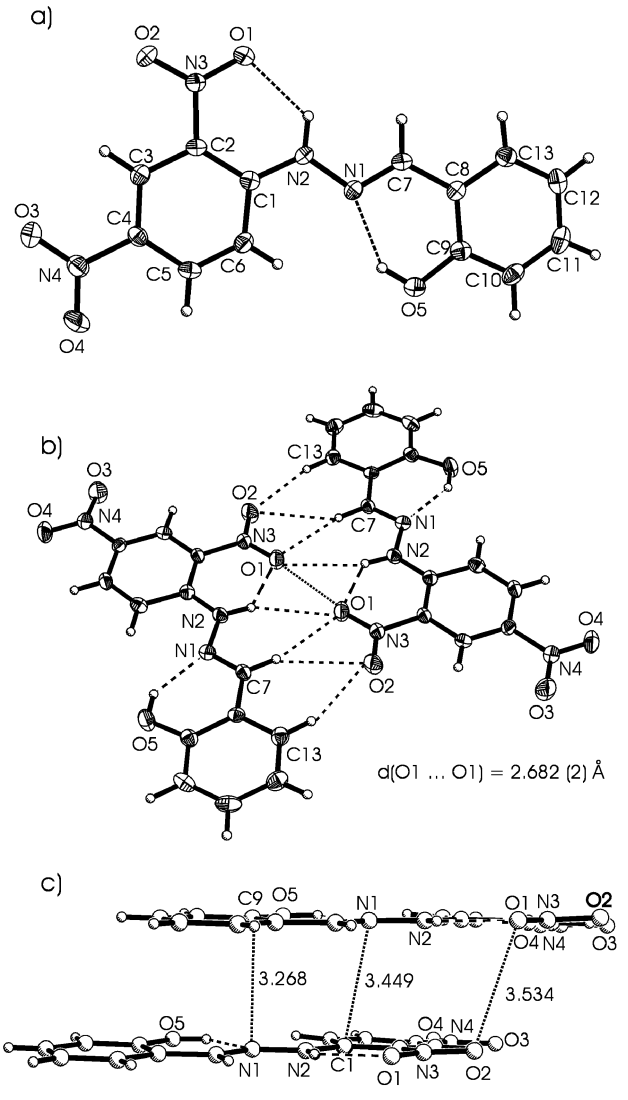

Fig. 1 (a) ORTEP diagram showing labelling scheme for compound **1** and thermal ellipsoids drawn at 50% probability level; (b) details of dimeric self-assembly; (c) inter-planar molecular arrangement with the shortest non-bonding contacts of an electrostatic nature.

vary considerably. These observations indicate that the aromatic character of the benzene ring is disturbed by abundance of the resonance form of 2,5-diene geometry (Scheme 3). The primary reason of such bond length variability is involvement of the hydrazone NH and *o*-NO_2 groups in the formation of an intramolecular, hydrogen-bonded, quasi-aromatic π-electron system shown in Scheme 3. This type of hydrogen bonding has been named by Gilli "the resonance assisted hydrogen bond (RAHB)".[23]

A similar mesomeric structure of the aromatic ring (*i.e.*, 2,5-diene) has been found to predominate in the solid state studies of aromatic Schiff bases synthesized from salicylaldehyde.[24,25] In our case, hydrazone **1** shows co-existence of two of the above RAHB systems [see Fig. 1(a)]. Recently, proton transfer

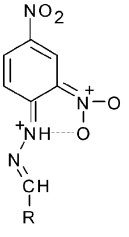

Scheme 3

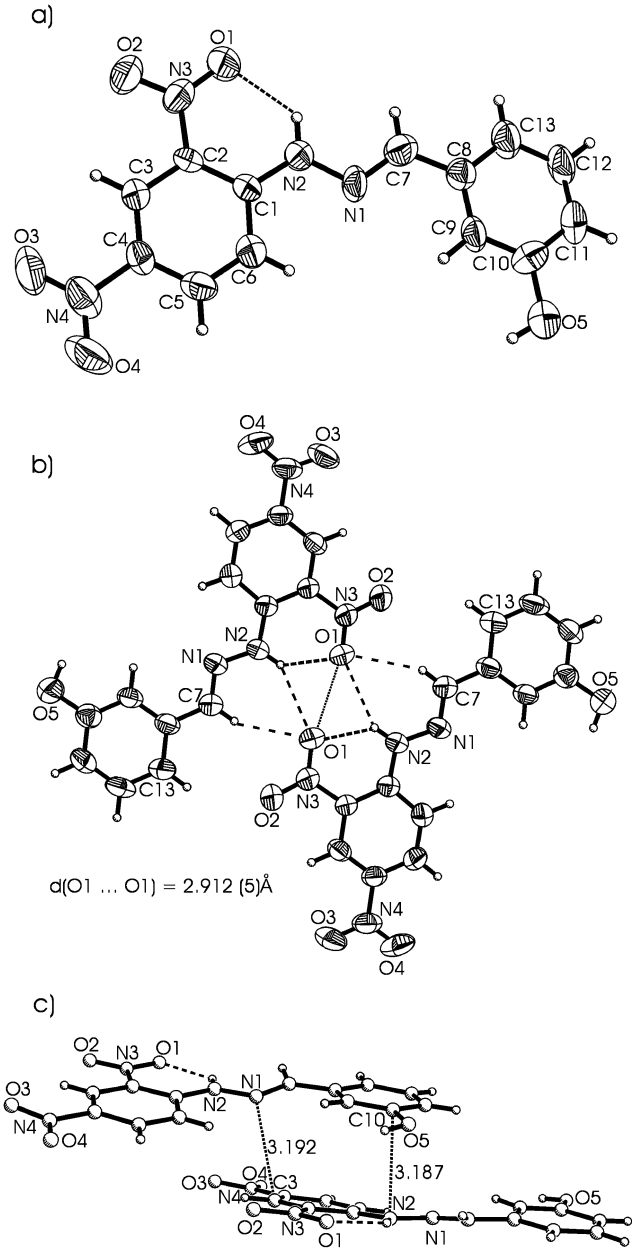

Fig. 2 (a) ORTEP diagram showing labelling scheme for compound **2** and thermal ellipsoids drawn at 50% probability level; (b) details of dimeric self-assembly; (c) inter-planar molecular arrangement with the shortest non-bonding distances of an electrostatic nature.

from phenol to the azomethine group N atom of the above Schiff bases, both in solution and in the solid state, has been observed.[26–28] Therefore, low temperature data were collected for compound **1** (measured at 200 K). Although residual density mapped on the least-squares plane of the molecule showed a second maximum located 0.78 Å from the imine nitrogen, refinement of the double occupancy model (0.83 : 0.17 ratio) was dubious.

Self-assembly of molecules and crystal packing

The title compounds were designed in such a way that contributions derived from hydrogen bonding and interactions between π-electron systems could be separated. In fact, the crystal packing is dominated by interactions between 2D networks built from intermolecularly hydrogen-bonded polar, aromatic molecules. According to the diagrams shown in Fig. 1(b)–4(b) for compounds **1**–**4**, respectively, the basic

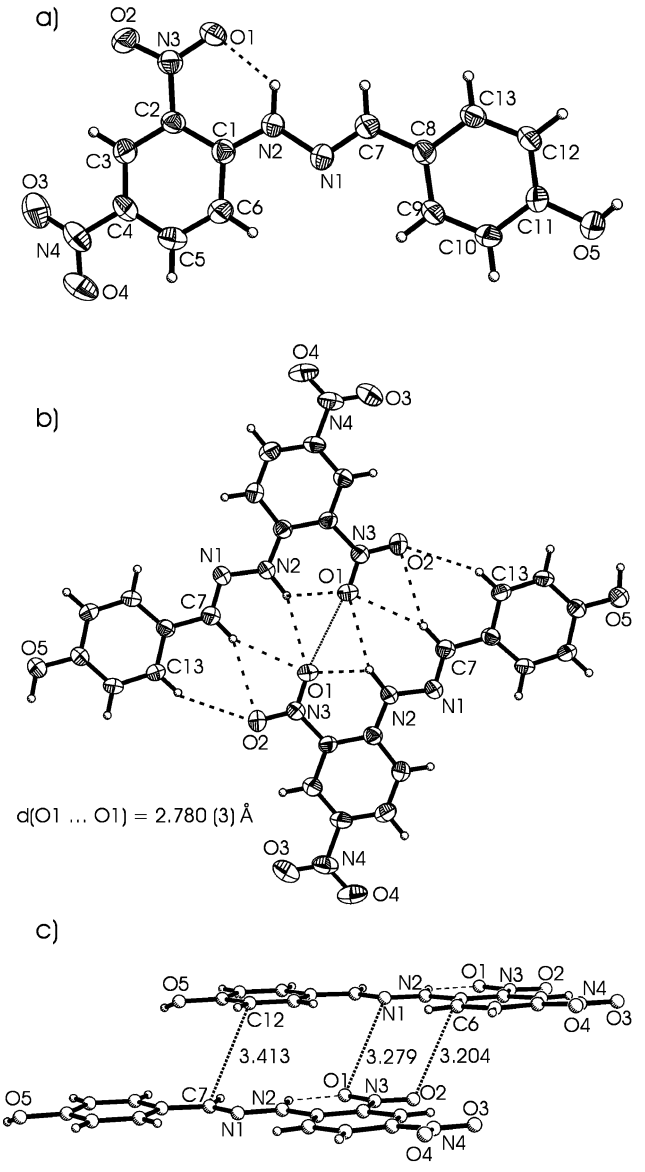

Fig. 3 (a) ORTEP diagram showing labelling scheme for compound **3** and thermal ellipsoids drawn at 50% probability level; (b) details of dimeric self-assembly; (c) inter-planar molecular arrangement showing the shortest non-bonding distances of an electrostatic nature and π-π stacking.

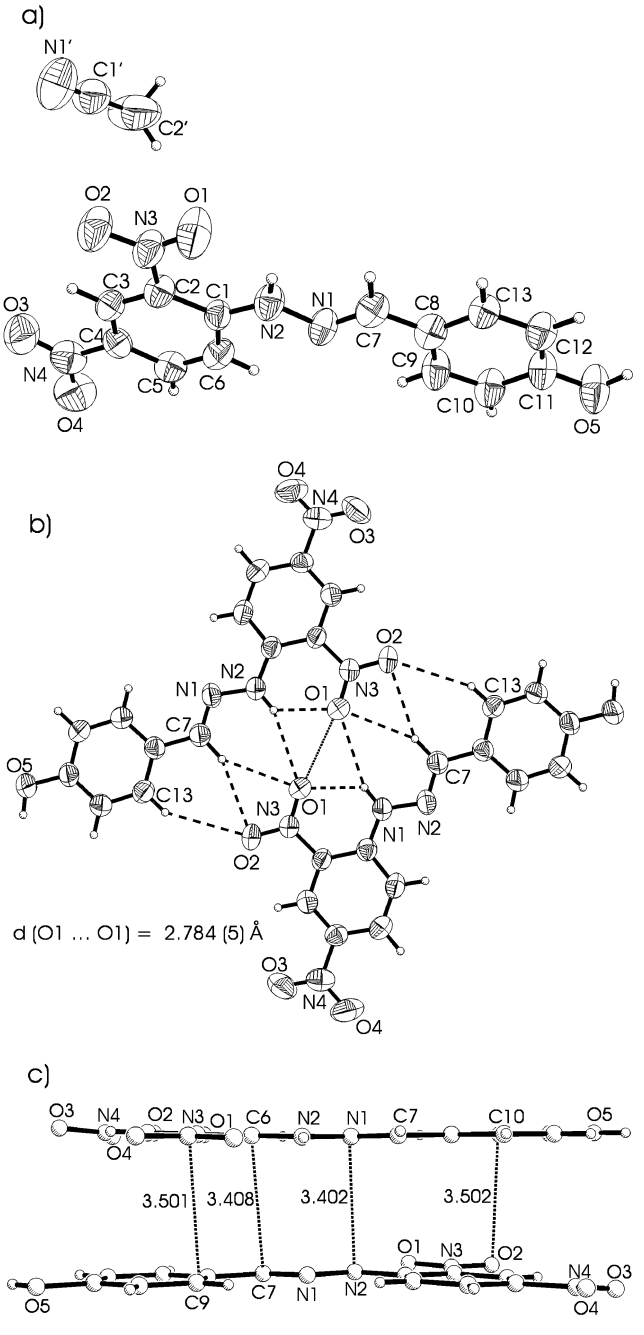

Fig. 4 (a) ORTEP diagram showing labelling scheme for compound **4** and thermal ellipsoids drawn at 50% probability level; (b) details of dimeric self-assembly; (c) inter-planar molecular arrangement showing the shortest non-bonding distances of an electrostatic nature.

recognition motif is a planar, centrosymmetric dimer. The geometries of the potential hydrogen bonds in the dimer along with those formed by OH groups are summarised in Table 3. For comparison, the sum of van der Waals radii for the respective N···O, C···O, H···O and H···N distances, considering criteria given by Bondi[29] and by Rowland and Taylor,[30] are given in Table 4. According to these, the strength and number of in-plane hydrogen bonds and inter-planar overlap between π-electron systems can be correlated. The weakest dimer, formed by molecules of **2**, provides the opportunity for the most efficient inter-planar stacking [see Table 3 and Fig. 1(c)–4(c)]. The remaining H···O nonbonding distances are in the range 2.57(3)–2.68(4) Å, satisfying both or at least Bondi's criteria. All donor–acceptor distances observed in the dimer exceed the sum of van der Waals radii. However, the whole system displays hydrogen bond characteristics: directionality, correlation between the strength of the hydrogen bond and the D–H···A angles and involvement of the C protons in typical **a** and **b** recognition patterns (Scheme 1). The main reason to consider these weak interactions as having attractive character is that the dimeric self-assembly is preserved even in the presence of competing hydrogen bonds formed by OH groups or inclusion of MeCN molecules (**4**). The cooperative action of the two NH···O and four to six CH···O hydrogen bonds creates "cohesive" forces between two small organic molecules. This employs oxygen electron pairs located both in *syn* and *anti* positions with respect to the C–N bond. The recognition pattern is a combination of three-centred $R_2^1(4)$ and $R_1^1(6)$ motifs according to the graph set assignments.[31] Moreover, formation of this supramolecular aggregate overcomes repulsion between symmetry-related O1 atoms in the dimer. The O1···O1 distances are in the range 2.683(2)–2.894(3) Å, far below the sum of the nonbonded contact radii adopted for oxygen—3.04 Å according to Bondi[29] or 3.12 Å according to Rowland and Taylor[30] [see Fig. 1(b)–4(b) and Table 4].

Querying the Cambridge Crystallographic Database provided information about $NO_2\cdots NO_2$ non-bonded interactions.

Table 2 Selected bond lengths (Å) and angles (°) for compounds **1**–**4**

	1	**2**	**3**	**4**
C(1)–N(2)	1.356(2)	1.354(4)	1.357(3)	1.348(4)
C(1)–C(2)	1.420(2)	1.412(4)	1.420(3)	1.425(4)
C(1)–C(6)	1.420(2)	1.414(4)	1.415(3)	1.409(4)
C(2)–C(3)	1.388(2)	1.385(4)	1.391(3)	1.385(4)
C(2)–N(3)	1.447(2)	1.445(4)	1.441(3)	1.437(4)
C(3)–C(4)	1.371(2)	1.367(4)	1.367(4)	1.362(4)
C(4)–C(5)	1.388(2)	1.388(5)	1.392(4)	1.388(4)
C(4)–N(4)	1.462(2)	1.449(4)	1.457(3)	1.451(4)
C(5)–C(6)	1.363(2)	1.361(5)	1.361(4)	1.361(5)
C(7)–N(1)	1.290(2)	1.276(4)	1.289(3)	1.277(4)
N(1)–N(2)	1.384(2)	1.364(4)	1.385(3)	1.379(3)
N(3)–O(1)	1.246(2)	1.229(3)	1.239(3)	1.235(3)
N(3)–O(2)	1.227(2)	1.217(3)	1.226(3)	1.220(3)
N(4)–O(3)	1.226(2)	1.210(4)	1.230(3)	1.220(4)
N(4)–O(4)	1.225(2)	1.218(4)	1.220(3)	1.230(4)
N(2)–C(1)–C(6)	120.5(1)	119.6(3)	120.1(2)	120.7(3)
N(2)–C(1)–C(2)	123.2(1)	123.8(3)	123.0(2)	123.2(3)
C(6)–C(1)–C(2)	116.2(1)	116.6(3)	116.9(2)	116.1(3)
C(3)–C(2)–C(1)	121.8(2)	121.9(3)	121.2(2)	121.4(3)
C(3)–C(2)–N(3)	115.9(1)	116.1(3)	116.1(2)	116.0(3)
C(1)–C(2)–N(3)	122.3(1)	122.0(3)	122.6(2)	122.6(3)
C(4)–C(3)–C(2)	118.8(1)	118.9(3)	119.0(2)	119.4(3)
C(3)–C(4)–C(5)	121.5(1)	121.1(3)	121.6(2)	121.4(3)
C(3)–C(4)–N(4)	118.7(1)	118.7(3)	118.9(3)	118.8(3)
C(5)–C(4)–N(4)	119.8(1)	120.2(3)	119.4(3)	119.8(3)
C(6)–C(5)–C(4)	119.8(2)	120.2(3)	119.7(3)	119.5(3)
C(5)–C(6)–C(1)	121.6(2)	121.2(3)	121.5(3)	122.2(3)
N(1)–C(7)–C(8)	122.0(1)	120.6(3)	121.5(2)	121.5(3)
C(7)–N(1)–N(2)	114.8(1)	115.8(3)	113.3(2)	114.6(3)
C(1)–N(2)–N(1)	120.1(1)	119.8(3)	119.3(2)	119.5(3)
O(2)–N(3)–O(1)	122.2(1)	122.3(3)	122.2(2)	121.2(3)
O(2)–N(3)–C(2)	119.1(1)	119.0(3)	119.1(2)	119.7(3)
O(1)–N(3)–C(2)	118.7(1)	118.8(3)	118.7(2)	119.1(3)
O(3)–N(4)–O(4)	123.5(1)	122.9(3)	123.8(3)	122.5(3)
O(3)–N(4)–C(4)	118.7(1)	119.2(3)	116.8(3)	119.7(3)
O(4)–N(4)–C(4)	117.8(1)	117.9(3)	119.4(3)	117.8(3)

Fig. 5 shows histograms of all O···O distances between NO_2 groups with the mean value located at *ca.* 3.3 Å. Interestingly, a subset of 100 compounds can be found where the above distance lies in the range 2.607–2.900 Å. This set contains 31 examples of a poly-nitro organic or organometallic compounds with $NO_2\cdots O_2N$ distances as short as 2.8 Å. Among them, only molecules of *aci*-nitrodiphenylmethane are involved in the formation of planar centrosymmetric dimers (Scheme 4) with O···O = 2.607 Å, as in carboxylic acids.[32]

In the remaining crystal structures nitro groups are not involved in classic hydrogen bonding and 3D networks are formed due to numerous electrostatic interactions between polar NO_2 groups and CH···O interactions. Two spatial arrangements of the NO_2 groups shown in Scheme 5 are observed: the recently found motif **I**, which allows overlap of the N–O dipoles (several short N···O contacts due to the parallel arrangement are observed)[33] and the equally abundant motif **II**, which allows attraction between the positively charged nitrogen and negatively charged oxygen atoms with simultaneous reduction of repulsion between oxygen atom lone pairs due to the quasi-perpendicular arrangement (one short and one long O···O contacts, Scheme 5). The second group represents 68 compounds of *o*-nitroaniline type (derivatives of 2,4,6-trinitroaniline, 2-nitrophenylhydrazone, and 2-nitrosemicarbazone) where the nitro group often is involved in an intramolecular RAHB system. As in our case, in the majority of crystal structures the recognition pattern **III** was found, with oxygen atoms approaching each other approximately along the N–O bond, affording O···O distances in the range 2.666–2.800 Å. In several cases strongly connected dimers of 2,4-dinitrophenylhydrazone molecules, synthesised from bulky groups bearing non-aromatic aldehydes or ketones, are also formed. According to circular scattergrams, showing directionality of the NO_2 group interactions and *ab initio* derived maps of potential energy calculated around a nitro group, the direction along the N–O bond is weakly

Table 3 Hydrogen bond geometry (in Å and °) in **1**–**4**

D–H···A		*d*(D–H)	*d*(H···A)	*d*(D···A)	∠(DHA)	Sym[a]
N(2)–H(2)···O(1) (RAHB)	**1**	0.96(1)	1.94(2)	2.615(2)	125.6(1)	#1
	2	0.83(4)	1.94(4)	2.609(4)	136(4)	#1
	3	1.01(1)	1.90(2)	2.615(3)	125(2)	#1
	4	0.87(3)	1.99(3)	2.624(4)	129(3)	#1
N(2)–H(2)···O(1) (dimer)	**1**	0.96(1)	2.50(2)	3.4164(2)	160.6(2)	#2
	2	0.83(4)	2.55(4)	3.240(4)	142(3)	#3
	3	1.01(1)	2.49(1)	3.425(3)	155(2)	#5
	4	0.87(3)	2.59(3)	3.395(4)	155(3)	#7
C(7)–H(7)···O(1) (dimer)	**1**	0.97(2)	2.65(2)	3.553(2)	155.0(1)	#2
	2	0.90(4)	2.68(4)	3.374(5)	135(3)	#3
	3	0.99(3)	2.57(3)	3.492(3)	156(2)	#5
	4	1.03(3)	2.62(3)	3.513(4)	145(2)	#7
C(7)–H(7)···O(2) (dimer)	**1**	0.97(2)	2.65(2)	3.549(2)	153.5(1)	#2
	2	0.90(4)	2.83(4)	3.499(4)	133(3)	#3
	3	0.99(3)	2.66(3)	3.558(3)	152(2)	#5
	4	1.03(3)	2.65(3)	3.553(5)	146(2)	#7
C(13)–H(13)···O(2) (dimer)	**1**	0.94(2)	2.68(2)	3.564(2)	156.4(1)	#2
	2	0.93	2.80	3.583(5)	142.2	#3
	3	0.93	2.64	3.506(3)	155.7	#5
	4	0.93	2.79	3.621(4)	148.5	#7
O(5)–H(5A)···N(1)	**1**	0.98(1)	1.86(1)	2.690(2)	139.7(2)	#1
O(3)	**2**	0.87(6)	2.52(6)	3.216(5)	138(5)	#4
O(4)		0.87(6)	2.44(6)	3.305(5)	171(5)	#4
O(3)	**3**	0.98(1)	1.82(5)	2.806(3)	175(4)	#6
O(3)	**4**	0.90	2.34	3.162(4)	151.8	#8
O(4)		0.90	2.18	2.982(4)	147.4	#8

[a] Symmetry transformations used to generate equivalent atoms: #1: x, y, z; #2: $-x+1, -y, -z$; #3: $-x+2, -y+1, -z+2$; #4: $-x+2, -y, -z+2$; #5: $-x+1, -y+1, -z$; #6: $x-1/2, -y+5/2, z-1/2$; #7: $-x+1/2, -y+1/2, -z+1$; #8: $x-1/2, -y-1/2, z-1/2$.

Table 4 Non-bonding contacts (Å)

	Bondi[16]	Rowland and Taylor[17]
N···O	3.07	3.17
C···O	3.22	3.31
O···H	2.72	2.65
N···H	2.75	2.70

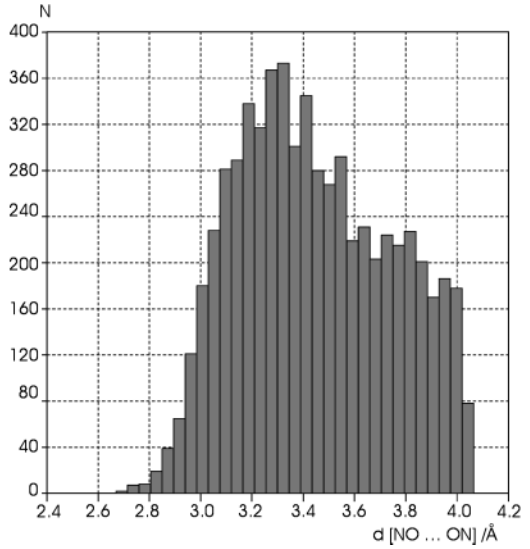

Fig. 5 Histograms of $NO_2\cdots O_2N$ non-bonding contacts with the mean value located around 3.3 Å.

populated by electrophiles.[13] Two effects might account for the increase of steric accessibility of nitro groups by nucleophiles: anisotropy of the oxygen atom valence sphere due to formation of a strong and directional intramolecular RAHB system, and the push–pull effect of numerous, weak hydrogen bonds formed within the dimer, possibly due to intermolecular RAHB.[34,35]

Several types of intermolecular hydrogen bonds formed by OH groups have been observed in the present structures: weak bifurcated (**2** and **4**) or single, relatively strong (**3**). Their presence modulates the geometry within the dimer and controls inter-planar overlapping of the polar groups. In the crystal of compound **1**, where no intermolecular H-bonded OH groups were found, the O1···O1 distance is the shortest—2.683(2) Å with only one inter-planar contact below the sum of van der Waals radii [Fig. 1(c)]. In compound **2** intermolecular OH···O hydrogen bonds are weak, the O1···O1 separation is the largest, but inter-planar adhesion is the strongest [Fig. 2(c)]. Compounds **3** and **4** with one and two relatively strong OH···O hydrogen bonds have the same O1···O1 contact

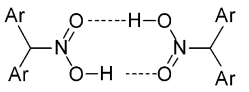

Scheme 4

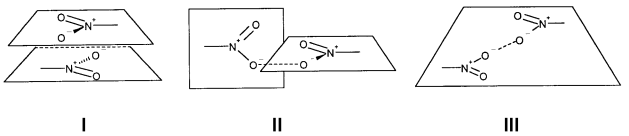

Scheme 5

Table 5 Selected FT-IR bands (cm^{-1}) for **1**, **2**, and **3**

		γ(NH)	γ(C=N)	$\gamma(NO_2)_{as}$	$\gamma(NO_2)_{sym}$
1	KBr	3270	1619	1588	1335
	$CHCl_3$	3292	1619	1600	1337
2	KBr	3290[a]	1616	1588	1329
	$CHCl_3$	3325	1617	1600	1336
3	KBr	3278	1618	1586	1330
	$CHCl_3$	3290	1617	1591	1333

[a] Twinned band.

distance, 2.780(3) Å, and approximately the same type of inter-planar interactions [Fig. 3(c) and 4(c)].

Two packing patterns are observed in the crystals: co-facial stacking of layers containing centrosymmetric dimers linked to each other by OH···O hydrogen bonds (compounds **2** and **3**) or a combination of face-to-edge located planes formed by dimers (compounds **1** and **4**).

FT-IR spectrometry

It was of interest to see if some structural characteristics observed in crystals of the title compounds can also be seen in solution. Table 5 shows selected bands in the vibrational spectra of **1**–**3** measured in KBr and in $CHCl_3$, for groups potentially taking part in the aggregation process. According to these data the C=N band is not sensitive to changes in the environment (crystal *versus* solution or involvement in an RAHB system, as in **1**). Positions of two characteristic bands for asymmetric and symmetric stretching vibrations of the NO_2 group depend on their non-bonding interactions and are shifted towards higher wave numbers when going from solid state to solution [$\Delta\nu(NO_2)_{as} = 5$–12 cm^{-1} and $\Delta\nu(NO_2)_{sym} = 2$–$7$ cm^{-1}]. As expected, the NH stretching band, (intra- and intermolecularly hydrogen bonded in crystals) on dissolution in $CHCl_3$ is moved upfield by 12–35 cm^{-1}. Comparison of the solid state geometry of the title compounds and a series of β-ketoarylhydrazones[36] (both containing a HN–N=C–C=O moiety involved in a RAHB system) shows that intramolecular hydrogen bonds in the former are weaker (D···A distances: 2.609(4)–2.624(4) Å *versus* 2.541(2)–2.615(3) Å for β-ketoarylhydrazones). Accordingly, ν(NH) stretching frequencies of compounds **1**–**4** are in the range 3270–3290 cm^{-1}, while these for β-ketoarylhydrazones are in the range 2950–3170 cm^{-1}. The above data confirm the weaker proton affinity of the NO_2 group oxygens. Stretching frequencies ν(NH) observed in $CHCl_3$ or dioxane are in the range for hydrogen-bonded NH groups (3200–3400 cm^{-1}), which can be attributed to molecular aggregation or and to preservation of the intramolecular RAHB system.

Conclusions

Classification of topologic requirements assessed to weak and strong hydrogen bonds is based on van der Waals contacts derived for atoms treated as hard spheres. This is confirmed by experimental solid state data stored in the CCD. Although this principle is statistically true, the Cambridge Crystallographic Database contains numerous examples of precisely determined structures of nitro compounds where intermolecular contacts between alike charged, non-hydrogen-bonded oxygen atoms are significantly shorter. In this work we demonstrated that multiple hydrogen bonding and other electrostatic interactions involving the nitro groups in several 2,4-dinitrophenyl hydrazones and other polynitro compounds, even if individually modest, can be used for molecular recognition of small organic molecules. To our knowledge, this is the first example

demonstrating this cooperative effect and particularly, the occurrence of resonance-assisted (intramolecular) hydrogen bonding can significantly anisotropise the electronic structure of a nitro group and allow much stronger penetration of atomic valence spheres during the recognition process. Multiple binding is the driving force behind protein folding, proton and electron-transfer processess, and aggregation of biomolecules. Therefore, the above observation can be important for understanding the efficient binding in biological hosts derivatised by the introduction of a nitro group, and explain the presence of unusually short contacts between polar groups.

References

1 G. R. Desiraju, *Angew. Chem., Int. Ed. Engl.*, 1995, **34**, 2311.
2 A. Nangia and G. R. Desiraju, *Top. Curr. Chem.*, 1998, **198**, 67.
3 G. R. Desiraju, *Crystal Engineering—The Design of Organic Solids*, Materials Science Monograph No. 54, Elsevier, Amsterdam, 1989.
4 G. R. Desiraju, *Science*, 1997, **278**, 404.
5 C. B. Aakeröy, *Acta Crystallogr., Sect. B*, 1997, **53**, 569.
6 A. Nangia and G. R. Desiraju, *Acta Crystallogr., Sect. A*, 1998, **54**, 934.
7 D. Braga, F. Grepioni and G. R. Desiraju, *Chem. Rev.*, 1998, **98**, 1375.
8 A. Gavezzotti and G. Filippini, *Chem. Commun.*, 1998, 287.
9 K. Müller-Dethlefs and P. Hobza, *Chem. Rev.*, 2000, **100**, 143.
10 A. Szumna, J. Jurczak and Z. Urbańczyk-Lipkowska, *J. Mol. Struct.*, 2000, **526**, 165.
11 T. W. Panunto, Z. Urbańczyk-Lipkowska, R. Johnson and M. C. Etter, *J. Am. Chem. Soc.*, 1987, **109**, 7786.
12 F. H. Allen, J. P. M. Lommerse, V. J. Hoy, J. A. K. Howard and G. R. Desiraju, *Acta Crystallogr., Sect. B*, 1997, **53**, 1006.
13 J. M. A. Robinson, D. Philp, K. D. M. Harris and B. M. Kariuki, *New J. Chem.*, 2000, **24**, 799.
14 F. H. Allen, C. A. Baalham, J. P. M. Lommerse, P. R. Raithby and E. Sparr, *Acta Crystallogr., Sect. B*, 1997, **53**, 1017.
15 F. H. Allen and O. Kennard, *Chem. Des. Autom. News*, 1993, **8**, 131.
16 E. Kangas and B. Tidor, *J. Phys. Chem.*, 2001, **105**, 880.
17 F. Vögtle and W. M. Müller, *Chem. Ber., Ger. Ed.*, 1980, **113**, 2081.
18 R. S. Tewari and P. Parihar, *J. Chem. Eng. Data*, 1981, **26**, 418.
19 M. Kidwai, R. Bala and K. C. Srivastava, *Indian J. Chem., Sect. B.*, 1994, **33**, 193.
20 B. Szczęsna and Z. Urbańczyk-Lipkowska, *Supramol. Chem.*, 2001, **13**, 247.
21 G. M. Sheldrick, SHELXS97, Program for Crystal Structure Solution, University of Göttingen, Germany, 1997.
22 G. M. Sheldrick, SHELXL97, Program for Crystal Structure Determination, University of Göttingen, Germany, 1997.
23 G. Gilli, F. Bellucci, V. Ferretti and V. Bertolasi, *J. Am. Chem. Soc.*, 1989, **111**, 1023.
24 T. Dziembowska, *Pol. J. Chem.*, 1998, **72**, 193.
25 K. Wozniak, H. He, J. Klinowski, W. Jones, T. Dziembowska and E. Grech, *J. Chem Soc., Faraday Trans.*, 1995, **91**, 77.
26 S. H. Alarcón, A. C. Olivieri, A. Nord and R. K. Harris, *J. Chem. Soc., Perkin Trans. 2*, 1996, 2293.
27 Z. Rozwadowski and T. Dziembowska, *Magn. Res. Chem.*, 1999, **37**, 274.
28 B. Kamieński, W. Schilf, T. Dziembowska, Z. Rozwadowski and A. Szady-Chełmieniecka, *Solid State NMR*, 2000, **16**, 285.
29 A. Bondi, *J. Phys. Chem.*, 1964, **68**, 441.
30 R. S. Rowland and R. Taylor, *J. Phys. Chem.*, 1996, **100**, 7384.
31 M. C. Etter, *Acc. Chem. Res.*, 1990, **23**, 120.
32 H. Bock, R. Dienelt, H. Schodel, Z. Havlas, E. Hertweck and W. A. Herrmann, *Angew. Chem., Int. Ed. Engl.*, 1993, **32**, 1758.
33 K. Wozniak, H. He, J. Klinowski, W. Jones and E. Grech, *J. Phys. Chem.*, 1994, **98**, 13 755.
34 V. Bertolasi, P. Gilli, V. Ferretti and G. Gilli, *Acta Crystallogr., Sect. B*, 1995, **51**, 1004.
35 V. Bertolasi, P. Gilli, V. Ferretti and G. Gilli, *Acta Crystallogr., Sect. B*, 1998, **54**, 50.
36 V. Bertolasi, P. Gilli, V. Ferretti, G. Gilli and K. Vaughan, *New J. Chem.*, 1999, **23**, 1261.